International Journal of Technology

http://ijtech.eng.ui.ac.id

Research Article

A High Selective and Sensitive Spectrophotometric Cholesterol Detection Using β-Cyclodextrin/Fe3O4 Composite as the Identification Agent

Vanya Fahira Dharmawan [1], Isnaini Rahmawati [1], Afiten Rahmin Sanjaya [1], Beti Ernawati Dewi [2], Endang Saepudin [1], Tribidasari Anggraningrum Ivandini [1*]

[1]*Department of Chemistry, Faculty of Mathematics and Natural Sciences, Universitas Indonesia, Depok, 16424, Indonesia*
[2]*Department of Microbiology, Faculty of Medicine, Universitas Indonesia, Depok, 16424, Indonesia*
[*]*Corresponding author: ivandini.tri@sci.ui.ac.id; Tel.: +62 21 7270027*

Abstract: This study aimed to develop a simple and low-cost cholesterol detection using UV-vis spectrophotometer with β-cyclodextrin (BCD)/Fe_3O_4 nanocomposite as the identification agent. Cholesterol detection was achieved by replacing methylene blue (MB) molecules, which formed inclusion complexes in BCD cavities. The results showed that cholesterol concentration could be determined from the released amount of MB detected by UV-vis spectrometer. To enhance the sensitivity of signal responses of the sensors, BCD was functionalized with citrate before being deposited on Fe_3O_4 magnetic nanoparticles. The characterization of the nanocomposite was performed by X-Ray-diffraction (XRD), Fourier Transform Infrared (FTIR) spectra, and Scanning Electron Microscope-Energy Dispersive X-Ray (SEM-EDX). The developed sensor showed linear responses (R^2<0.99) toward cholesterol concentrations in the range between 0 and 100 µM, with a sensitivity of 0.56 x 103 a.u. M^{-1} and estimated detection limit of 7.71 µM. Comparison with the previous detections using the electrochemical method showed that the performance of the developed sensor was comparable. Furthermore, by applying the optimum parameters, including pH solution of 7.4, contact time of 10 min, and composite weight of 3% containing 3% citrate-modified BCD, the developed sensor successfully analyzed cholesterol concentrations in human serum samples.

Keywords: Cholesterol; β-cyclodextrin; Fe_3O_4; Methylene blue; Non-enzymatic sensor

1. Introduction

Cholesterol is produced by animal cells for biosynthesis of bile acids, precursors of steroid hormones, and vitamin D as well as the main component of lipoproteins (Li et al., 2019; Dinh and Thompson, 2016; Vučić and Cvetković, 2016). High levels of cholesterol can form plaque capable of narrowing and blocking the artery lumen. This condition causes blood flow restriction to the heart and potentially ruptures arteries, triggering angina, stroke, and heart attack (Dhawane et al., 2019; Rahman and Woollard, 2017). Therefore, monitoring the level of cholesterol in the blood is considered important as an initial step to prevent cardiovascular disease.

This work was supported by the 'Ministry of Education and Culture, Directorate General of Higher Education, Indonesia funded by 'PDUPT Grant and No. NKB-890/UN2.RST/HKP.05.00/2023',

https://doi.org/10.14716/ijtech.v16i2.7176
Received September 2024; Revised October 2024; Accepted January 2025

Various analytical methods have been developed for cholesterol detections, including the conventional Liebermann-Burchard reaction, gas and liquid chromatography, surface plasmon resonance, as well as electrochemical methods (Putri et al., 2024; Lukito et al., 2024; Nor et al., 2023; Derina et al., 2018; Albuquerque et al., 2016; Chen et al., 2015; Arya et al., 2007). The electrochemical methods are established as the most popular for cholesterol biosensors, comprising cholesterol oxidase or esterase enzymes (Ahmadraji and Killard, 2016; Mondal et al., 2014; Gomathi et al., 2011; Basu et al., 2007). Despite the significant potential, the activities of enzymes are strongly influenced by temperature, pH, and other chemicals. Therefore, a non-enzymatic cholesterol sensor is considered as a better alternative method to be developed (Ariyanta et al., 2021; Chen et al., 2020; Derina et al., 2020; Willyam et al., 2020; Agnihotri et al., 2015).

A selective non-enzymatic sensor for cholesterol can be developed by using the specific reaction between cholesterol and β-cyclodextrin (BCD) nanocomposites (Nasution et al., 2023; Willyam et al., 2020; Zidovetzki and Levitan, 2007). BCD is an oligosaccharide consisting of seven glucose units bound in a cyclic manner with a hydrophobic inner cavity and a hydrophilic outer cavity. This nanocomposite is reported to bind selectively with cholesterol through hydrophobic site (Nasution et al., 2023; Willyam et al., 2020). However, BCD and cholesterol do not have any specific colour or any electrochemically active properties. Therefore, to produce signals in the measurements of cholesterol levels, a mediator with such properties is required. An example of compounds that can be used as a mediator is methylene blue (MB) because it can provide interaction with BCD. Initially, BCD is conditioned to form the inclusion complexes with MB. When cholesterol is added, MB that has interacted with BCD would be expelled since cholesterol has a better binding affinity. In previous studies, the electrochemical properties of MB were used to produce signals in the form of oxidation current of MB (Nasution et al., 2023; Willyam et al., 2020). BCD was immobilized on Fe_3O_4 nanoparticles to separate BCD more easily from the system, leaving a solution containing the released MB. Apart from magnetic properties, Fe_3O_4 has good thermal and electrical properties as well as the ability to amplify signals and increase the selectivity of cholesterol biosensors (Yadav et al., 2021; Willyam et al., 2020). MB is also a colored aromatic organic compound capable of absorbing light and generating color in the visible region. The detection of MB can be performed using spectrophotometry (Khan et al., 2022; Mohadi et al., 2022).

This study continues our previous investigation to develop a selective non-enzymatic sensor for cholesterol, using the specific and competitive reaction between cholesterol to BCD and methylene blue to BCD. First, a modification of the hydroxyl group of BCD with citrate was carried out to increase the binding affinity for cholesterol and improve the sensor performance (Wu et al., 2021; Willyam et al., 2020; Ogoshi and Harada, 2008). Second, the use of UV-Visible spectrometry to detect methylene blue that expelled from BCD when cholesterol was added. The use of a UV-vis spectrophotometer in this study offers several advantages, including a higher sensitivity allowing for the detection of low cholesterol concentrations, Additionally, UV-vis spectrophotometry is easy to use with minimal sample preparation requirements, making the analysis become more simple and rapid (Fatah et al., 2023).

Based on the results, the developed sensor showed that the modification of BCD with citrate affects the contact time between BCD and cholesterol. A linear correlation between the responses toward cholesterol concentrations was achieved in the concentration range from 0 to 100 μM. Additionally, comparable performance was obtained by the developed sensor using visible spectrometry method in comparison with the similar electrochemical method. Further applications of the developed sensors successfully were shown to analyze cholesterol concentration in human serum samples. This showed the potential of sensors for real applications to detect cholesterol.

2. Methods

2.1. Materials

In this study, BCD, citric acid monohydrate ($C_6H_8O_7$), and cholesterol ($C_{27}H_{46}O$) were obtained from Sigma-Aldrich US. Other material including MB ($C_{16}H_{18}N_3SCl$) was obtained by Wako Japan. Ferric chloride hexahydrate ($FeCl_3.6H_2O$), ferrous chloride tetrahydrate ($FeCl_2.4H_2O$), dipotassium phosphate (K_2HPO_4), potassium dihydrogen phosphate (KH_2PO_4), ammonium hydroxide (NH_4OH), isopropanol, n-hexane, ethanol absolute, and methanol were supplied by Merck US. All solutions were prepared using doubled distilled water produced by Millipore Direct-Q® 5 UV.

2.2. Synthesis and Characterization of BCD/Fe_3O_4 and BCD-CIT/Fe_3O_4

Fe_3O_4 magnetic nanoparticles, BCD/Fe_3O_4, and CIT-BCD/Fe_3O_4 composites were synthesized using the coprecipitation method. Initially, salt precursors of Fe^{2+} and Fe^{3+} ions (1:2 ratio) were used to precipitate metal oxides in alkaline solution, containing ammonia which acted as the precipitating agent to form $Fe(OH)_2$ and $Fe(OH)_3$(Khan et al., 2022; Yadav et al., 2021). A total of 5 grams of $FeCl_3.6H_2O$ and 2 grams of $FeCl_2.4H_2O$ were dissolved in 100 mL of BCD or citrate-modified BCD (CIT-BCD) solution, followed by stirring at 80°C for 10 min. Ammonia solution was carefully dripped until pH of the solution reached 11-12. After vigorously stirring the solution for 30 min at the same temperature, the precipitate was separated with an external magnet, washed with water and methanol, and dried at 60°C for a day before used (Willyam et al., 2020). This precipitate was labeled as BCD/Fe_3O_4 and CIT-BCD/Fe_3O_4.

Prior to the synthesis of CIT-BCD/Fe_3O_4, the CIT-BCD was prepared by esterification reaction via cyclic anhydride, where the hydroxyl group on the macromolecule reacts with the carboxyl group of citric acid (Domínguez-Renedo et al., 2023). Meanwhile, the CIT-BCD was synthesized by dissolving 1.5 g BCD and 0.55 g citric acid in 10 mL water and stirred at 80°C for 3 h. Then, the mixture was centrifuged to separate the solution from the precipitate. The precipitate was washed with isopropanol for 3 times and the obtained white precipitate was dried at 60°C for 24 hours (Jayaprabha and Joy, 2015).

The composites were characterized by using FTIR Spectrometer (Bruker ALPHA II Compact FTIR) and X-Ray Diffraction (Malvern PANalytical Aeris at 40 kV and 80 mA with Co-Kα radiation (λ = 0.179 nm). The morphological structure of composites was performed with Scanning Electron Microscope (FEI Quanta 650 FEG). The UV-Vis Spectra were taken using a Thermo Scientific™ Multiskan™ GO.

2.3. Cholesterol Measurements

Before cholesterol measurements, some parameters, including pH, amount of the composite, and the contact times between cholesterol and composites, were investigated to obtain the optimum conditions. Firstly, MB 500 μM solution was prepared in pH variations of 6.2, 6.6, 7.0, 7.4, and 7.8 PBS 0.1 M solution. Each solution was added dropwise at 10 µL on the microplate. Subsequently, the microplate was covered and the absorbance was measured using UV-Vis spectrophotometer with a wavelength of 300-800 nm.

MB was immersed in BCD/Fe_3O_4 and BCD-CIT/Fe_3O_4 by dissolving 2 mL of 60 µM MB solution with 3 mL of composites dispersed in 0.1 M phosphate buffer solution (PBS) pH 7.4 for 3 h. Next, the MB-modified BCD/Fe_3O_4 (MB/BCD/Fe_3O_4) and MB-modified CIT-BCD/Fe_3O_4 (MB/CIT-BCD /Fe_3O_4) were separated with external magnets and washed with water (Willyam et al., 2020).

To determine the cholesterol content, 3% (w/t) MB/BCD/Fe_3O_4 and 3% (w/t) MB/CIT-BCD/Fe_3O_4 composites have been dissolved with 0.1 M PBS in an Eppendorf tube with the addition of 60 µM MB with 1:1 (v/v) ratio (Willyam et al., 2020). Then, 100 µL of standard solution of cholesterol was added to the mixture while shaking and allowed to stand for 10

min with MB/BCD/Fe_3O_4 and 15 min with MB/BCD-CIT/Fe_3O_4. The mixture of composites was separated using external magnet, and 10 µL of the solution was dripped on the microplate to determine the absorbance using UV-Vis spectrophotometry. The additional MB was used to meet the detection limit of the spectroscopy detection.

2.4. Sample Preparation

Cholesterol level was measured using human blood plasma obtained from the Faculty of Medicine, University of Indonesia, Jakarta, Indonesia. After consent was confirmed, 3 mL of blood was drawn from a healthy subject and placed in an EDTA tube. A volume of 20 µL of EDTA plasma was placed in an Eppendorf tube, followed by the adding 200 µL of methanolic KOH. The tube was incubated in a water bath at 37- 40℃ for 55 min. After cooling to room temperature, 400 µL of n-hexane and 200 µL of water were added and the tube was centrifuged at 3500 rpm for 5 min. The upper aqueous layer was transferred to another test tube for analysis using the developed method (Li et al. 2019).

The validation method was performed using LC200 High Performance Liquid Chromatography (HPLC). HPLC system was equipped with UV detector applied at the operating wavelength of 212 nm. A mixture of methanol and ethanol (70:30, v/v) was used as the mobile phase with a flow rate of 1 ml min^{-1} at room temperature.

In this study, three variations of cholesterol measurement conditions were performed for each nanocomposite. These included variations in the type and weight of the nanocomposite, including variations in the contact time. Each variation of BCD/Fe_3O_4 and BCD-CIT/Fe_3O_4 nanocomposites was dissolved in 0.1M PBS solution with a weight ratio of 2% (w/w). Approximately 400 µL of nanocomposites were placed into an Eppendorf tube, added with 100 µL of 100 µM MB solution. Furthermore, the nanocomposites were separated to obtain the solution using an external magnet, and its initial absorbance was measured. A total of 100 µL of 100 µM cholesterol standard solution was added into the Eppendorf tube, shaken, and left for 15 min. The nanocomposite was separated with an external magnet and the solution was collected to determine its final absorbance.

Table 1 Number of receptors in each container

Experiment	Container	Receptor
1	50	28
2	100	14
3	150	9
4	200	7
5	250	5

3. Results and Discussion

3.1. Synthesis and characterization of BCD/Fe_3O_4 and CIT-BCD/Fe_3O_4

Synthesis of Fe_3O_4 showed the formation of black precipitate when pH system reached around 11 to 12. The comparison of FTIR Spectra of the precipitate in Figure 1(a) showed that similar peaks were observed at BCD before and after modification. The peak at 1028 cm^{-1}, 1152 cm^{-1}, 2919 cm^{-1}, and 3398 cm^{-1} were attributed to the asymmetric stretch of C-O-C, the symmetric stretch of C-O-C and C-H as well as the symmetric and asymmetric stretching of the -OH groups, respectively (Abarca et al., 2015; Wang et al., 2014). However, modification of a new peak observed at 1171 cm^{-1} was attributable to the C=O groups of the carboxylic acid in citric acid. The peak shifting from 1732 cm^{-1} to 1171 cm^{-1} was due to the C=O stretching because of ester formation from carboxylic (Nasution et al., 2023; Agnihotri et al., 2015).

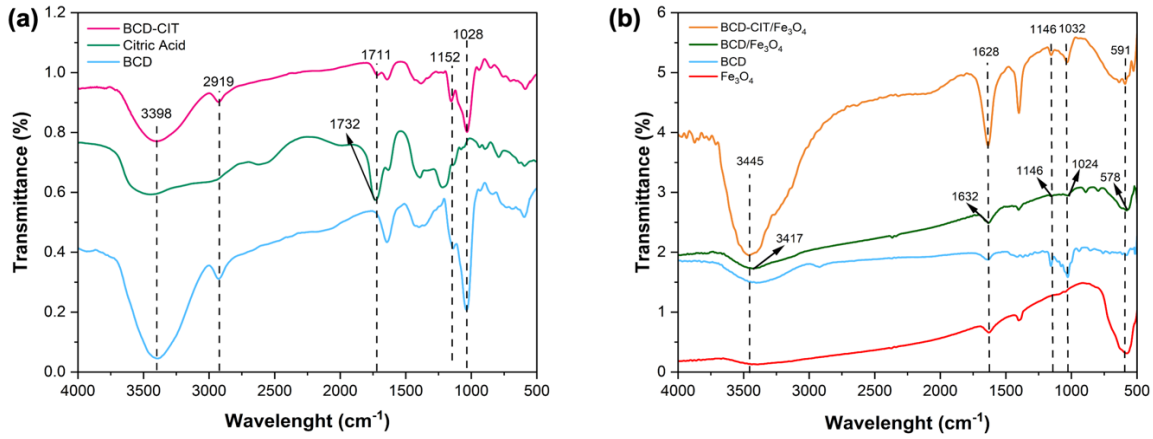

Figure 1 Comparison of FTIR Spectra of (a) BCD before and after citrate modification, and (b) Fe_3O_4 before and after modification with BCD and citrate

FTIR spectra of the unmodified Fe_3O_4 indicated by red line in Figure 1(b) shows a main peak at 591 cm^{-1} attributed to Fe-O vibrations of Fe_3O_4. Small peaks at 1628 cm^{-1} and 3445 related to O-H bending and stretching are also observed (Saepudin et al., 2021; Azizi, 2020). After modification with BCD as indicated by green line in Fig1(b), new peaks at 1024 cm^{-1}, 1146 cm^{-1} are observed due to C-O-C stretching and C-C/C-O bending vibrations of BCD, respectively (Abarca et al., 2015; Wang et al., 2014). These peaks are also observed in the spectra of the unmodified BCD (Figure 1(b), blue line) (Guo et al., 2015).

In the case of modification with CIT-BDD (Figure 1(b), orange line), similar peaks to BCD/Fe_3O_4 are also observed. However, these peaks are significantly sharper compared to BCD/Fe_3O_4 as the citrate groups contain more C=O groups (ester form) of CIT-BCD. A significant increase in the peak intensity was observed at around 3400 cm^{-1} due to the interaction between CIT-BCD and Fe_3O_4. The results indicated that BCD and BCD-CIT were successfully immobilized on Fe_3O_4.

Figure 2 shows that XRD patterns of Fe_3O_4, BCD/Fe_3O_4, and BCD-CIT/Fe_3O_4 can be matched to the Bragg reflections proportional to the standard phase of the spinal structure of Fe_3O_4 (JCPDS: 19-0629). The peaks of Fe_3O_4 were 35.17 (220), 41.47 (311), 50.71 (400), 63.24 (422), 67.57 (511), and 74.52 (440). The diffraction of BCD/Fe_3O_4 were 35.08 (220), 41.43 (311), 50.56 (400), 62.68 (422), 67.40 (511), and 74.44 (440), while BCD-CIT/Fe_3O_4 had 35.00 (220), 41.50 (311), 50.51(400), 63.08 (422), 67.60 (511), and 74.40 (440).

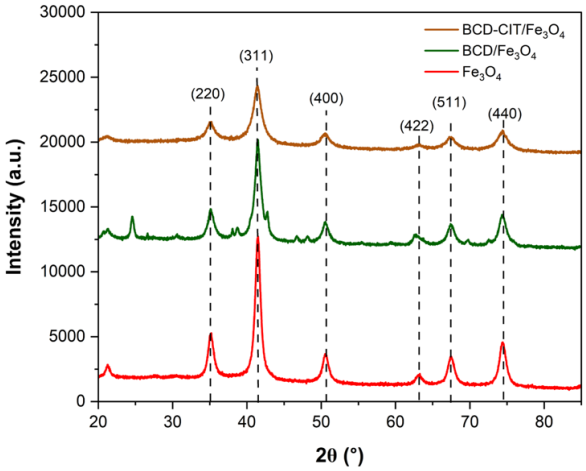

Figure 2 XRD spectra of Fe_3O_4, BCD/Fe_3O_4, and CIT-BCD/Fe_3O_4

The enhancement in intensity indicates an increasing level of crystallinity in the composites. The mono lattice crystal sizes of Fe_3O_4 in Fe_3O_4, BCD/Fe_3O_4, and BCD-CIT/Fe_3O_4 were determined by Scherrer equation, which showed 8.58 nm, 11.53 nm, and 13.42 nm, respectively. Both composites have a specific peak of Fe_3O_4 confirming successful immobilization on BCD and BCD-CIT (Guo et al., 2015).

SEM characterization (Figure 3) was conducted to identify the morphology and homogeneity of CIT-Fe_3O_4. The results showed that the prepared CIT-Fe_3O_4 had a spherical shape that mostly aggregated to the inhomogeneous large particles. Further Energy Dispersive X-Ray (EDX) spectra showed that the weight composition of Fe and O was approximately 49.7 and 38.0 %(w/w), respectively. These values were equivalent to the atomic ratio of approximately 1:3. More amount of oxygen in Fe_3O_4 composition indicated that the modification with BCD and CIT was successfully performed. The element composition of CIT-BCD/Fe_3O_4 measured by EDX results is summarized in Table 1.

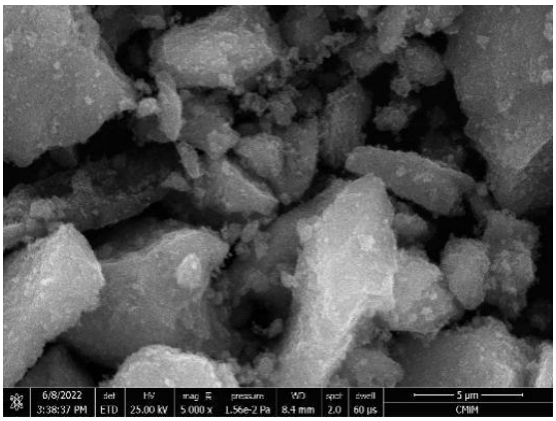

Figure 3 SEM image of the prepared CIT-Fe_3O_4 at 5000-times magnifications

Table 1 Element composition of Fe_3O_4 determined by using EDX

Element	Weight %	Atomic %
Fe	46.80	18.76
O	38.40	53.65
C	14.80	27.59

3.2. UV-vis spectrophotometer Measurements of Methylene Blue

UV-vis spectrophotometer of 60 µM MB in 0.1 M PBS solution pH 7.4 (Figure 4(a), blue line) shows a shoulder and main absorbance peak at 609 nm and 664 nm, respectively. This shows the presence of MB dimer and monomer, respectively (Khan et al., 2022). The dimeric species between two MB molecules and the aggregation from the interaction with H_2O molecules can cause a hypochromic shift, with an absorption peak from 664 nm to 609 nm (Timotius et al., 2022; Florence and Naorem, 2014). Meanwhile, the presence of 0.1 M PBS solution as the solvent at a certain pH is capable of changing the optical properties of MB due to an electrostatic interaction between MB and 0.1 M PBS solution. This process causes bathochromic shift and produces different absorbance intensities (Ariyanta et al., 2024; Grante et al., 2014). The bathochromic shift is also accompanied by a hyperchromic effect or an increase in absorption intensity (Florence and Naorem, 2014; Grante et al., 2014). The largest intensity of the MB peaks in this study was observed at pH 7.4 (Figure 4(b)).

The detection of cholesterol was performed by measurements of MB concentration released from the composites after mixed with the samples. The addition of a sample containing cholesterol into the composite caused the release of MB proportional to the concentration of cholesterol due to a higher affinity of cholesterol to BCD than MB (Nasution et al., 2023; Willyam et al., 2020). The mechanism of cholesterol detection is described in

Figure 5 together with the typical spectra of MB before (green line) and after (orange line) contacting MB-BCD/Fe_3O_4 and MB-CIT-BCD/Fe_3O_4 with 60 µM cholesterol. A higher intensity of the peak at 664 nm after contact with the composite was observed in the spectra, showing the release of MB. Additionally, a slightly higher absorbance intensity at the lower wavelength was observed, indicating the presence of other materials. The figure confirms the successful detection of MB in the system.

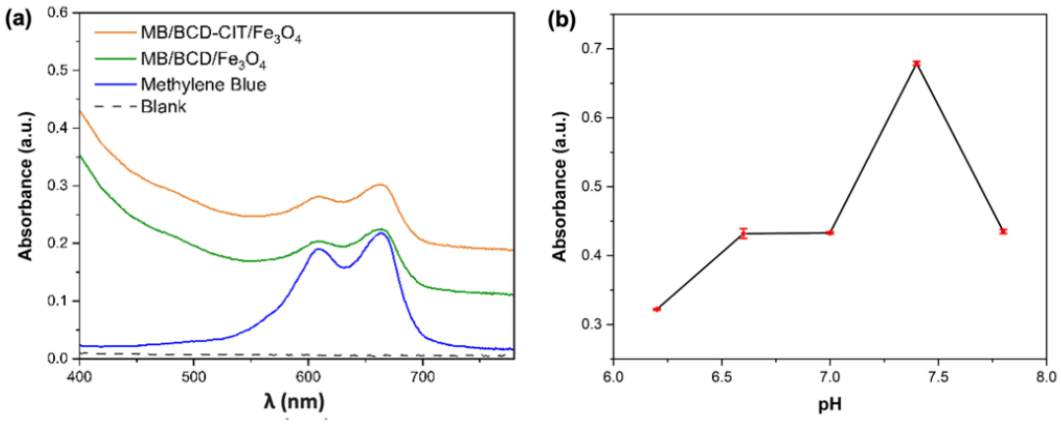

Figure 4 (a) The absorbance spectrum of 60 µM MB in 0.1M PBS pH 7.4 compared to the typical spectra of the released MB from MB/BCD/Fe_3O_4 and MB/CIT-BCD/Fe_3O_4 after 15-min contact to the sample containing 60 µM cholesterol

The maximum absorbance of the standard solution after the treatment with the composite was achieved at 3% of BCD and 3% of CIT-BCD, as shown in Figure 6(a) and 6(b), respectively. Meanwhile, the various weights used were saturated at 3% weight of composites, as shown in Figure 6(c) and 6(d). Observation at different optimum contact times showed that BCD/Fe_3O_4 required approximately 15 min contact time to achieve maximum MB release. BCD-CIT/Fe_3O_4 required only 10 min as shown in Figure 6(e) and 6(f), respectively. The results indicated faster kinetics of cholesterol adsorption at CIT-BCD/Fe_3O_4 than BCD/Fe_3O_4. This suggests that the presence of citrate groups stabilizes the loading of BCD on the surface of Fe_3O_4, increasing cholesterol affinity to composite. A previous report based on the electrochemical detection of MB also showed better performance when using CIT-BDD due to higher affinity with cholesterol (Nasution et al., 2023).

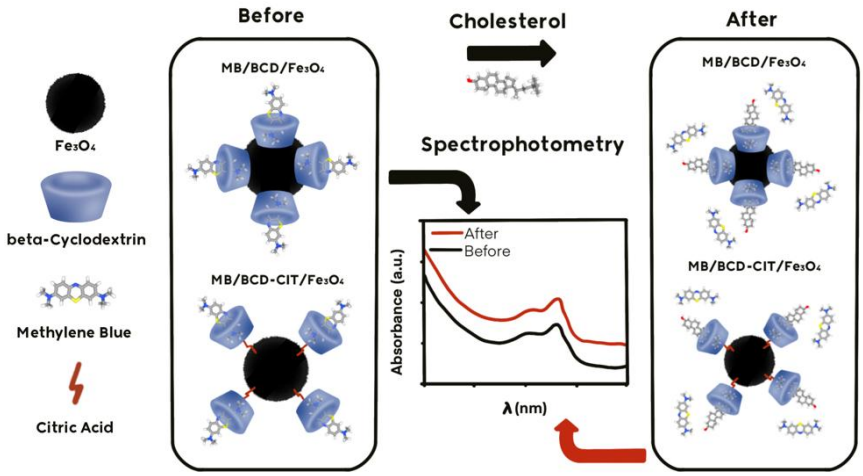

Figure 5 Illustration of the typical mechanisms of the sensor after the addition of sample containing cholesterol

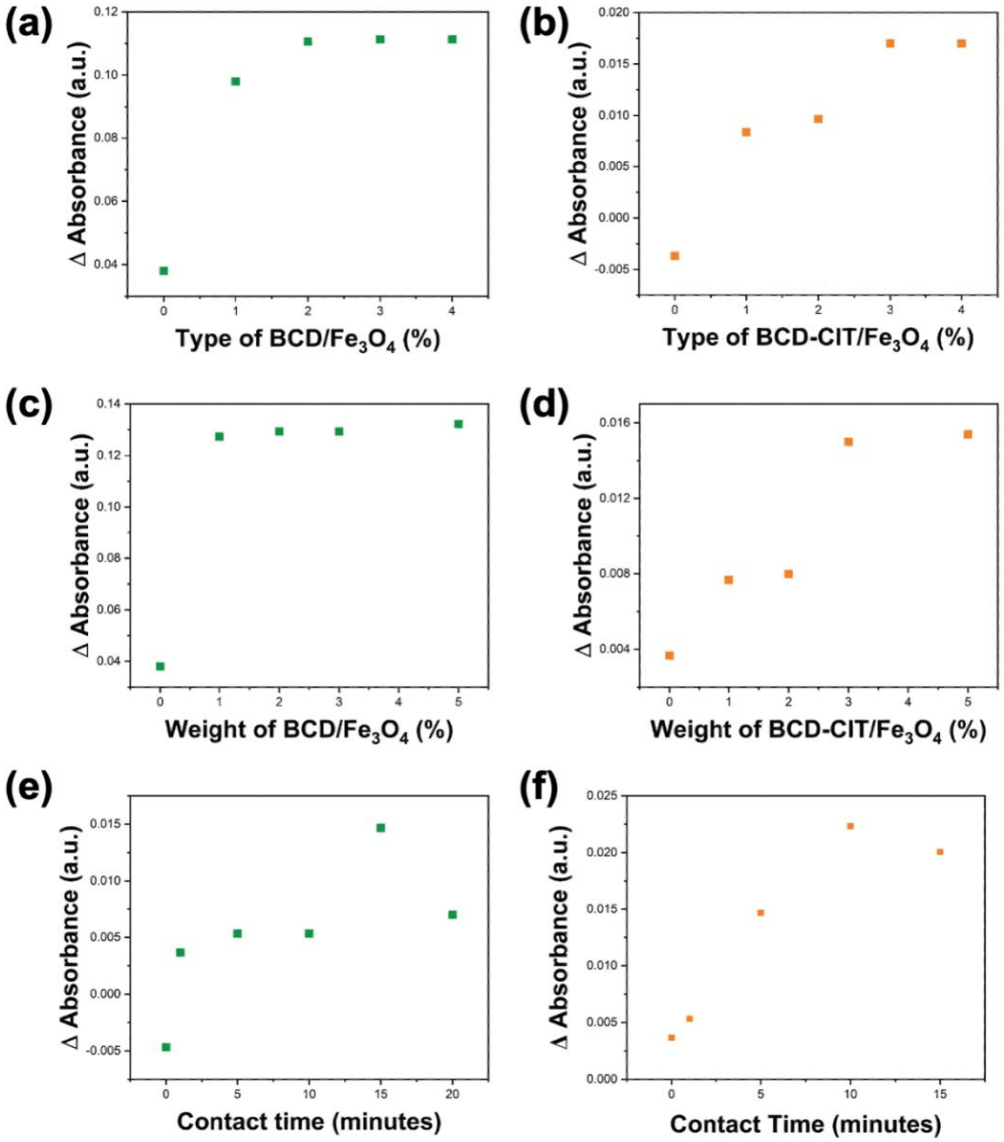

Figure 6 Comparison of the absorbance changes of the released MB from MB/BCD/Fe_3O_4 and MB/BCD/Fe_3O_4, respectively, after 15-min contact with the solutions containing 60 µM standard cholesterol at (a-b) various concentrations of BCD, (c-d) various weights of composites, and (e-f) various contact times

Based on these results, 3% of BCD content with 3% of composite weight were fixed for the next experiments to detect cholesterol using 15 min and 10 min contact times for BCD/Fe_3O_4 and CIT-BCD/Fe_3O_4, respectively. The optimization of cholesterol measurement conditions was 3% (w/t) MB/BCD(3%)/Fe_3O_4 with 15 min and 3% (w/t) MB/CIT-BCD(3%)/Fe_3O_4 10 min contact time.

3.3. The Detection of Cholesterol using UV-Vis Spectrophotometer

The optimum parameters of the composite were used to obtain a linear calibration curve of cholesterol in the concentration range from 0 to 100 µM. Figures 7 and 8 indicated that the MB released from BCD/Fe_3O_4 and CIT-BCD/Fe_3O_4 composites, after contacting with cholesterol, were proportional to the concentration of cholesterol. This was shown by a high linear correlation between the absorption intensity of MB and the concentrations of

cholesterol with R^2 of around 0.99. However, 2 times higher sensitivity of CIT-BCD/Fe_3O_4 (560 a.u. M^{-1}) than BCD/Fe_3O_4 (280 a.u. M^{-1}) was observed.

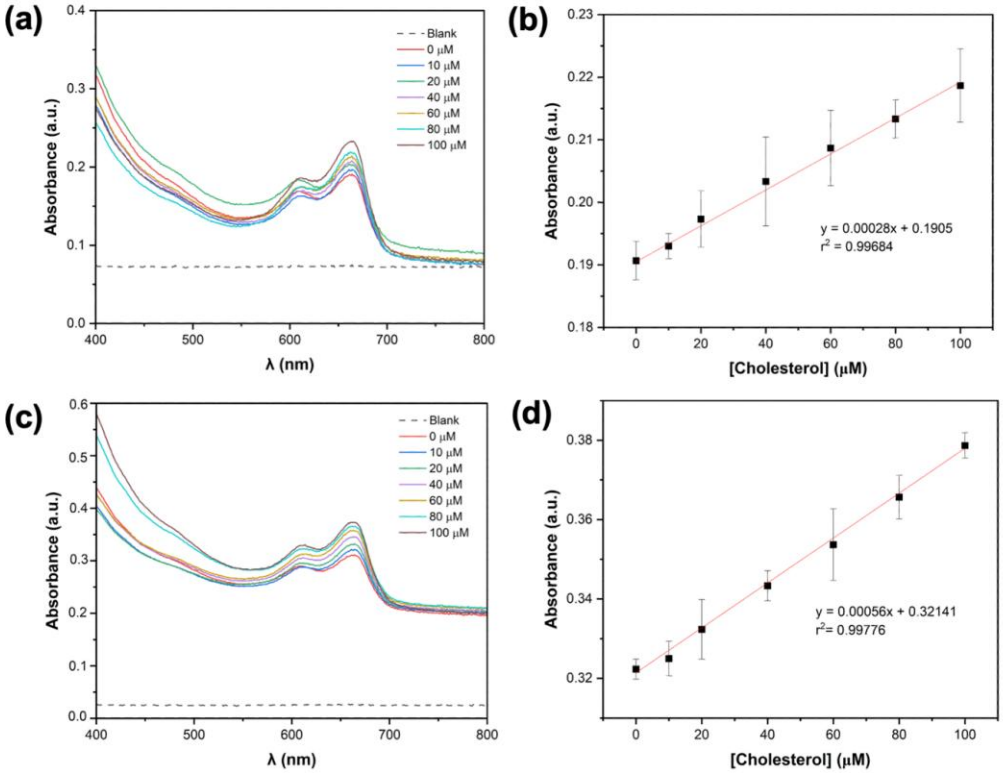

Figure 7 The absorbance spectra and calibration curves of the released MB from (a-b, respectively) MB/BCD/Fe_3O_4 and (c-d, respectively) MB/CIT-BCD/Fe_3O_4 after 15-min contact with the solutions containing 60 μM standard cholesterol

Table 2 Analytical performances of the developed method

Parameters	Materials	
	BCD/Fe_3O_4	CIT-BCD/Fe_3O_4
λ (nm)	664	664
Beer's law limit (μM)	8.16 - 100	7.71 - 100
Sensitivity (a.u. M^{-1})	0.28 x 10^3	0.56 x 10^3
Detection limits (μM)	8.16	7.71
Quantification limits (μM)	27.21	25.70
Response time (min)	15	10
Regression equation		
Slope (μM)	0.00028	0.00056
Intercept	0.19	0.32
Correlation coefficient (r^2)	0.99	0.99

Better limit of detection (LOD) and limit of quantification (LOQ) at 7.71 μM and 25.21 μM could be achieved when using CIT-BCD/Fe_3O_4. The values obtained were 8.16 μM and 27.21 μM when using BCD/Fe_3O_4. The results indicated that the spectrophotometric sensor using CIT-BCD/Fe_3O_4 has the potential to be developed, as presented in Table 1. Moreover, the comparison of the proposed sensor performance against other reported cholesterol sensors in Table 2 shows comparable detection capabilities to other previously developed sensors, particularly among various methods.

Sensor repeatability tests were conducted on the BCD/Fe_3O_4 and CIT-BCD/Fe_3O_4 to further monitor the stability of the measurements. Figures 9 (a) and (b) showed that incorporating citrate molecules into the BCD improved the stability of the measurements

with a relative standard deviation (RSD) of 4.42% compared to the system without citrate (RSD: 6.72%). This suggested that better interaction between cholesterol molecules with the BCD/Fe_3O_4 system improved the release of MB molecules and enhanced the stability of cholesterol/BCD/Fe_3O_4 complexes. The results showed better repeatability of the measurements, which was consistent with the suggested mechanism in Figure 5.

Table 3 Comparison methods of cholesterol with literature

Method	Sensor	Linear Range (μM)	LOD (μM)
Fluorescence	BCD-AuNCs (Xiao et al., 2022)	10 - 100	5.77
	SH-β-CD-AUNCS(Liu et al., 2024)	20 - 150	16.07
	N-GQDs/CrPic	0 - 520	0.4
Amperometry	MB/BCD/Fe_3O_4(Willyam et al., 2020)	2.88 - 150	2.88
	MB/BCD-CIT/Fe_3O_4(Nasution et al., 2023)	0 - 100	3.93
Spectrophotometry	ChOx/GQDs-TMB-H_2O_2(Nirala et al., 2015)	20 - 600	6
	MB/BCD/Fe_3O_4 (This work)	0 - 100	8.16
	MB/BCD-CIT/Fe_3O_4(This work)	0 - 100	7.71

The selectivity of cholesterol sensors was examined by comparing the detection of cholesterol (CL) standard solutions with and without the presence of interfering agents, such as palmitic acid (C16:0), dexamethasone (DEX), glucose (Glu), arginine (R), phenylalanine (P), and tyrosine (T). Figure 9(c) shows that the presence of interfering agent caused a less significant effect on the signal responses of the BCD/Fe_3O_4. A maximum decrease of the responses to 0.45% in the presence of glucose and arginine, respectively, were observed. Meanwhile, a slight increase was shown at 0.44% for palmitic acid, dexamethasone, phenylalanine, and tyrosine.

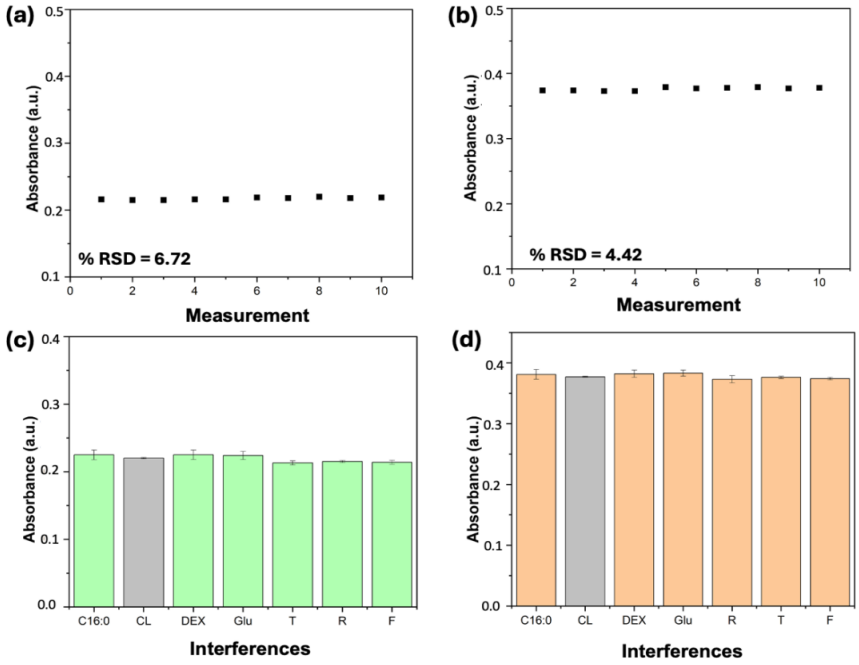

Figure 9 The plots of the absorbance spectra from the released MB from MB/BCD/Fe3O4 and MB/CIT-BCD/Fe3O4, respectively, after 15-min contact with the solutions containing 60 μM standard cholesterol (CL) in the absence (a-b) and the presence (c-d) of several potential interfering

agents, including palmitic acid (C16:0), dexamethasone (DEX), glucose (Glu), arginine (R), phenylalanine (P), and tyrosine (T)

As shown in Figure 9(d), the responses slightly decreased by approximately 2.9% and 0.3% in the presence of palmitic acid and arginine, respectively. The presence of glucose increased the response by 1.3%, while dexamethasone, phenylalanine, and tyrosine caused a rise of approximately 0.3%-0.8%. Less influence of these compounds indicated that both types of composites had good selectivity for cholesterol detections.

3.3. Real Sample Measurement

The performance of the developed sensor was assessed by measuring cholesterol content in EDTA blood plasma sample obtained from the Faculty of Medicine, Universitas Indonesia, Jakarta, Indonesia. Ethical clearance was obtained from the Health Research Ethics Committee, Faculty of Medicine Universitas Indonesia No. 878//UN2.F1/ETIK/PPM.00.03/2020. The results of cholesterol levels in EDTA blood plasma samples were 4000.00 μM and 4533.33 μM using BCD/Fe_3O_4 and BCD-CIT/Fe_3O_4 nanocomposite, respectively. The validation calculation was measured by HPLC analysis and obtained cholesterol concentration of 4540.00 μM. Furthermore, % recovery was calculated by comparing cholesterol obtained by developed sensor with HPLC results. As shown in Table 4, the recovery of cholesterol is between 88% and 100%, indicating the potential of the developed sensor as a promising analytical tool.

Table 4 Comparison of measurement results using HPLC and UV-Vis spectrophotometer in EDTA Blood Plasma

Methods		[Cholesterol] (mM)	% Recovery
HPLC		4.540	-
UV-Vis spectrophotometer	BCD/Fe_3O_4	4.000	88.11
	BCD-CIT/Fe_3O_4	4.533	99.85

4. Conclusions

In conclusion, this study showed that BCD/Fe_3O_4 and CIT-BCD/Fe_3O_4 MB nanocomposites were synthesized and characterized for the identification agents in cholesterol detection. MB released after the contact with cholesterol sample was detected by using UV-vis spectrophotometer at 664 nm. Applying 3% (w/w) BCD (3%)/Fe_3O_4 in 15 min contact time and 3% (w/w) CIT-BCD (3%)/Fe_3O_4 in 10 min contact time were found as the optimum conditions. Although good linearity in concentration ranging from 0 to 100 μM could be demonstrated by both nanocomposites, the developed cholesterol sensors using CIT-BCD/Fe_3O_4 showed better limit of detection, accuracy, and selectivity than BCD/Fe_3O_4 nanocomposite. The composites also successfully demonstrated the detection of EDTA-treated blood plasma samples. The results indicated that the developed sensor using CIT-BCD/Fe_3O_4 combined with the spectroscopy transducer was applicable for the detection of cholesterol.

Acknowledgements

This study was funded by the Ministry of Education and Culture, Directorate General of Higher Education, Indonesia, Hibah PDUPT 2023 with Contract No. NKB-890/UN2.RST/HKP.05.00/2023.

Author Contributions

Vanya Fahira Dharmawan: Writing – original draft, visualization, software, investigation, formal analysis, and data curation. **Isnaini Rahmawati**: formal analysis, data curation and writing – review & editing. **Afiten R. Sanjaya**: Visualization, validation, software, investigation, formal analysis, and data curation. **Beti Ernawati Dewi**: Formal analysis, data curation and writing – review & editing. **Endang Saepudin**: Writing – review & editing, methodology, and supervision. **Tribidasari A. Ivandini**: Writing – review & editing, validation, resources, methodology, supervision, conceptualization, and project administration.

Conflict of Interest

There are no conflicts of interest to declare.

References

Abarca, RL, Rodríguez, FJ, Guarda, A, Galotto, MJ & Bruna, JE 2015, 'Characterization of beta-cyclodextrin inclusion complexes containing an essential oil component', *Food Chemistry*, vol. 196, pp. 968-975, https://doi.org/10.1016/j.foodchem.2015.10.023

Agnihotri, N, Chowdhury, AD & De, A 2015, 'Non-enzymatic electrochemical detection of cholesterol using β-cyclodextrin functionalized graphene', *Biosensors and Bioelectronics*, vol. 63, pp. 212-217, https://doi.org/10.1016/j.bios.2014.07.037

Ahmadraji, T & Killard, AJ 2016, 'Measurement of total cholesterol using an enzyme sensor based on a printed hydrogen peroxide electrocatalyst', *Analytical Methods*, vol. 8, pp. 2743-2749, https://doi.org/10.1039/C6AY00468G

Albuquerque, TG, Oliveira, MBPP, Sanches-Silva, A & Costa, HS 2016, 'Cholesterol determination in foods: Comparison between high performance and ultra-high performance liquid chromatography', *Food Chemistry*, vol. 193, pp. 18-25, https://doi.org/10.1016/j.foodchem.2014.09.109

Ariyanta, HA, Ivandini, TA & Yulizar, Y 2021, 'Poly(methyl orange)-modified NiO/MoS_2/SPCE for a non-enzymatic detection of cholesterol', *FlatChem*, vol. 29, 100285, https://doi.org/10.1016/j.flatc.2021.100285

Ariyanta, HA, Nainggolan, H, Denti, SA, Segara, Y, Setiyanto, CM, Mayrosa, I & Ivandini, TA 2024, 'Garlic-induced stable black gold nanostructure: Optical, morphological, antibacterial, antioxidant and cytotoxic properties', *International Journal of Technology*, vol. 15, no. 4, pp. 965-975, https://doi.org/10.14716/ijtech.v15i4.6147

Arya, SK, Solanki, PR, Singh, SP, Kaneto, K, Pandey, MK, Datta, M & Malhotra, BD 2007, 'Poly-(3-hexylthiophene) self-assembled monolayer based cholesterol biosensor using surface plasmon resonance technique', *Biosensors and Bioelectronics*, vol. 22, no. 11, pp. 2516-2524, https://doi.org/10.1016/j.bios.2006.10.011

Azizi, A 2020, 'Green synthesis of Fe_3O_4 nanoparticles and its application in preparation of Fe_3O_4/cellulose magnetic nanocomposite: A suitable proposal for drug delivery systems', *Journal of Inorganic and Organometallic Polymers and Materials*, vol. 30, no. 9, pp. 3552-3561, https://doi.org/10.1007/s10904-020-01500-1

Basu, AK, Chattopadhyay, P, Roychoudhuri, U & Chakraborty, R 2007, 'Development of cholesterol biosensor based on immobilized cholesterol esterase and cholesterol oxidase on oxygen electrode for the determination of total cholesterol in food samples', *Bioelectrochemistry*, vol. 70, no. 2, pp. 375-379, https://doi.org/10.1016/j.bioelechem.2006.05.006

Chen, Y, Yang, G, Gao, S, Zhang, L, Yu, M, Song, C & Lu, Y 2020, 'Highly rapid and non-enzymatic detection of cholesterol based on carbon nitride quantum dots as fluorescent nanoprobes', *RSC Advances*, vol. 10, no. 65, pp. 39596-39600, https://doi.org/10.1039/D0RA07495K

Chen, YZ, Kao, SY, Jian, HC, Yu, YM, Li, JY, Wang, WH & Tsai, CW 2015, 'Determination of cholesterol and four phytosterols in foods without derivatization by gas chromatography-tandem mass spectrometry', *Journal of Food and Drug Analysis*, vol. 23, no. 4, pp. 636-644, https://doi.org/10.1016/j.jfda.2015.01.010

Derina, K, Korotkova, E & Barek, J 2020, 'Non-enzymatic electrochemical approaches to cholesterol determination', *Journal of Pharmaceutical and Biomedical Analysis*, vol. 191, 113538, https://doi.org/10.1016/j.jpba.2020.113538

Derina, K, Korotkova, E, Taishibekova, Y, Salkeeva, L, Kratochvil, B & Barek, J 2018, 'Electrochemical nonenzymatic sensor for cholesterol determination in food', *Analytical and Bioanalytical Chemistry*, vol. 410, no. 20, pp. 5085-5092, https://doi.org/10.1007/s00216-018-1164-x

Dhawane, M, Deshpande, A, Jain, R & Dandekar, P 2019, 'Colorimetric point-of-care detection of cholesterol using chitosan nanofibers', *Sensors and Actuators B: Chemical*, vol. 281, pp. 72-79, https://doi.org/10.1016/j.snb.2018.10.060

Dinh, T & Thompson, L 2016, 'Cholesterol: Properties, processing effects, and determination', *Encyclopedia of Food and Health*, pp. 60-69, https://doi.org/10.1016/B978-0-12-384947-2.00150-1

Domínguez-Renedo, O, Navarro-Cuñado, AM & Alonso-Lomillo, MA 2023, 'Electrochemical devices for cholesterol detection', *Journal of Pharmaceutical and Biomedical Analysis*, vol. 224, 115195, https://doi.org/10.1016/j.jpba.2022.115195

Fatah, FRAA, Rahmawati, I, Gunlazuardi, J & Sanjaya, AR 2023, 'Synthesis and characterization silica-MB@GO-NH_2 particle as fluorescence-based chlorine sensor', *Environmental and Materials*, vol. 1, no. 2, pp. 1-8, https://doi.org/10.61511/eam.v1i2.2023.399

Florence, N & Naorem, H 2014, 'Dimerization of methylene blue in aqueous and mixed aqueous organic solvent: A spectroscopic study', *Journal of Molecular Liquids*, vol. 198, pp. 255-258, https://doi.org/10.1016/j.molliq.2014.06.030

Gomathi, P, Ragupathy, D, Choi, JH, Yeum, JH, Lee, SC, Kim, JC, Lee, SH & Ghim, HD 2011, 'Fabrication of novel chitosan nanofiber/gold nanoparticles composite towards improved performance for a cholesterol sensor', *Sensors and Actuators B: Chemical*, vol. 153, no. 1, pp. 44-49, https://doi.org/10.1016/j.snb.2010.10.005

Grante, I, Actins, A & Orola, L 2014, 'Protonation effects on the UV/Vis absorption spectra of imatinib: A theoretical and experimental study', *Spectrochimica Acta Part A: Molecular and Biomolecular Spectroscopy*, vol. 129, no. 1, pp. 326-332, https://doi.org/10.1016/j.saa.2014.03.059

Guo, Z, Li, Y, Pan, S & Xu, J 2015, 'Fabrication of Fe_3O_4@cyclodextrin magnetic composite for the high-efficient removal of Eu(III)', *Journal of Molecular Liquids*, vol. 206, pp. 272-277, https://doi.org/10.1016/j.molliq.2015.02.034

Jayaprabha, KN & Joy, PA 2015, 'Citrate modified β-cyclodextrin functionalized magnetite nanoparticles: A biocompatible platform for hydrophobic drug delivery', *RSC Advances*, vol. 5, no. 28, pp. 22117-22125, https://doi.org/10.1039/C4RA16044D

Khan, I, Saeed, K, Zekker, I, Zhang, B, Hendi, AH, Ahmad, A, Ahmad, S, Zada, N, Ahmad, H, Shah, LA, Shah, T & Khan, I 2022, 'Review on methylene blue: Its properties, uses, toxicity and photodegradation', *Water*, vol. 14, no. 2, pp. 242-272, https://doi.org/10.3390/w14020242

Li, LH, Dutkiewicz, EP, Huang, YC, Zhou, HB & Hsu, CC 2019, 'Analytical methods for cholesterol quantification', *Journal of Food and Drug Analysis*, vol. 27, no. 2, pp. 375-386, https://doi.org/10.1016/j.jfda.2018.09.001

Liu, X, Yang, Z, Liu, J, Xiao, W & Li, H 2024, 'A detection system for serum cholesterol based on the fluorescence color detection of beta-cyclodextrin-capped gold nanoclusters', *Spectrochimica Acta Part A: Molecular and Biomolecular Spectroscopy*, vol. 308, pp. 1-10, https://doi.org/10.1016/j.saa.2023.123769

Lukito, AA, Tyrayoh, M, Prasetyanto, EA & Rukmini, E 2024, 'Development of sweat and saliva glucose sensors as alternative for non-invasive blood glucose monitoring', *International Journal of Technology*, vol. 15, no. 3, pp. 720-731, https://doi.org/10.14716/ijtech.v15i3.5535

Mohadi, R, Siregar, PMSBN, Palapa, NR & Lesbani, A 2022, 'Preparation of Zn/Al-chitosan composite for the selective adsorption of methylene blue dye in water', *Makara Journal of Science*, vol. 26, no. 2, pp. 128-136, https://doi.org/10.7454/mss.v26i2.1313

Mondal, K, Ali, MA, Agrawal, VV, Malhotra, BD & Sharma, A 2014, 'Highly sensitive biofunctionalized mesoporous electrospun TiO_2 nanofiber-based interface for biosensing', *ACS Applied Materials and Interfaces*, vol. 6, no. 4, pp. 2516-2527, https://doi.org/10.1021/am404931f

Nasution, MAF, Firmanti, MI, Riyanto, HG, Sanjaya, AR, Saepudin, E & Ivandini, TA 2023, 'Electrochemical and computational studies of citrate-modified β-cyclodextrin@Fe_3O_4 nanocomposite as a nonenzymatic sensor for cholesterol', *Sensors and Materials*, vol. 35, no. 12, pp. 4215-4234, https://doi.org/10.18494/SAM4698

Nirala, NR, Abraham, S, Kumar, V, Bansal, A, Srivastava, A & Saxena, PS 2015, 'Colorimetric detection of cholesterol based on highly efficient peroxidase mimetic activity of graphene quantum dots', *Sensors and Actuators B: Chemical*, vol. 218, pp. 42-50, https://doi.org/10.1016/j.snb.2015.04.091

Nor, MSM, Khan, AA, Mohamad, S & Thirunavakkarasu, P 2023, 'Development of optical fiber sensor for water salinity detection', *International Journal of Technology*, vol. 14, no. 6, pp. 1247-1255, https://doi.org/10.14716/ijtech.v14i6.6650

Ogoshi, T & Harada, A 2008, 'Chemical sensors based on cyclodextrin derivatives', *Sensors*, vol. 8, no. 8, pp. 4961-4982, https://doi.org/10.3390/s8084961

Putri, IZD, Jiwanti, PK, Supriyanto, G, Savitri, INI, Kurnia, KA, Setyaningsih, W, Yuliarto, B & Darmawan, N 2024, 'Highly sensitive aspartame electrochemical sensor in beverage samples using glassy carbon electrode modified with boron-doped nanodiamond/ZnO nanoparticles composite', *International Journal of Technology*, vol. 15, no. 5, pp. 1271-1281, https://doi.org/10.14716/ijtech.v15i5.5948

Rahman, MS & Woollard, K 2017, 'Atherosclerosis', *Advances in Experimental Medicine and Biology*, vol. 1003, pp. 121-144, https://doi.org/10.1007/978-3-319-57613-8_7

Saepudin, E, Yuliani, T, Nasution, MAF, Khalil, M, Hong, JW & Ivandini, TA 2021, 'Hemoglobin-modified core-shell Fe_3O_4@Au nanostructures for the electrochemical detection of acrylamide', *Makara Journal of Science*, vol. 25, no. 3, pp. 127-134, https://doi.org/10.7454/mss.v25i3.1232

Timotius, D, Kusumastuti, Y, Omar, R, Harun, R, Kamal, SMM, Jenie, SNA & Petrus, HTBM 2022, 'The study of methylene blue loading into chitosan-graft-maleic sponges', *International Journal of Technology*, vol. 13, no. 8, https://doi.org/10.14716/ijtech.v13i8.6133

Vučić, V & Cvetković, Z 2016, 'Cholesterol: Absorption, function and metabolism', *Encyclopedia of Food and Health*, pp. 47-52, https://doi.org/10.1016/B978-0-12-384947-2.00151-3

Wang, X, Luo, Z & Xiao, Z 2014, 'Preparation, characterization, and thermal stability of β-cyclodextrin/soybean lecithin inclusion complex', *Carbohydrate Polymers*, vol. 101, pp. 1027-1032, https://doi.org/10.1016/j.carbpol.2013.10.042

Willyam, SJ, Saepudin, E & Ivandini, TA 2020, 'β-Cyclodextrin/Fe_3O_4 nanocomposites for an electrochemical non-enzymatic cholesterol sensor', *Analytical Methods*, vol. 12, no. 27, pp. 3454-3461, https://doi.org/10.1039/D0AY00933D

Wu, H, Fang, F, Wang, C, Hong, X, Chen, D & Huang, X 2021, 'Selective molecular recognition of low-density lipoprotein based on β-cyclodextrin coated electrochemical biosensor', *Biosensors*, vol. 11, no. 7, pp. 216-226, https://doi.org/10.3390/bios11070216

Xiao, W, Yang, Z, Liu, J, Chen, ZC & Li, H 2022, 'Sensitive cholesterol determination by β-cyclodextrin recognition based on fluorescence enhancement of gold nanoclusters', *Microchemical Journal*, vol. 175, pp. 107625-107634, https://doi.org/10.1016/j.microc.2021.107125

Yadav, HM, Park, JD, Kang, HC & Lee, JJ 2021, 'Recent development in nanomaterial-based electrochemical sensors for cholesterol detection', *Chemosensors*, vol. 9, no. 5, pp. 98-117, https://doi.org/10.3390/chemosensors9050098

Zidovetzki, R & Levitan, I 2007, 'Use of cyclodextrins to manipulate plasma membrane cholesterol content: Evidence, misconceptions and control strategies', *Biochimica et Biophysica Acta*, vol. 1768, no. 6, pp. 1311-1324, https://doi.org/10.1016/j.bbamem.2007.03.026